

UCSF

UC San Francisco Previously Published Works

Title

Deep immunophenotyping reveals endometriosis is marked by dysregulation of the mononuclear phagocytic system in endometrium and peripheral blood

Permalink

<https://escholarship.org/uc/item/614557fk>

Journal

BMC Medicine, 20(1)

ISSN

1741-7015

Authors

Vallvé-Juanico, Júlia

George, Ashley F

Sen, Sushmita

et al.

Publication Date

2022-12-01

DOI

10.1186/s12916-022-02359-4

Copyright Information

This work is made available under the terms of a Creative Commons Attribution License, available at <https://creativecommons.org/licenses/by/4.0/>

Peer reviewed

RESEARCH ARTICLE

Open Access



Deep immunophenotyping reveals endometriosis is marked by dysregulation of the mononuclear phagocytic system in endometrium and peripheral blood

Júlia Vallvé-Juanico^{1,2}, Ashley F. George^{3,4†}, Sushmita Sen^{1,5†}, Reuben Thomas⁶, Min-Gyoung Shin⁶, Divyashree Kushnoor^{7,8}, Joshua J. Vásquez⁹, Kim Chi Vo¹, Juan C. Irwin¹, Nadia R. Roan^{3,4}, Alexis J. Combes^{7,8,9,10†} and Linda C. Giudice^{1*†}

Abstract

Background: Endometriosis is a chronic, estrogen-dependent disorder where inflammation contributes to disease-associated symptoms of pelvic pain and infertility. Immune dysfunction includes insufficient immune lesion clearance, a pro-inflammatory endometrial environment, and systemic inflammation. Comprehensive understanding of endometriosis immune pathophysiology in different hormonal milieu and disease severity has been hampered by limited direct characterization of immune populations in endometrium, blood, and lesions. Simultaneous deep phenotyping at single-cell resolution of complex tissues has transformed our understanding of the immune system and its role in many diseases. Herein, we report mass cytometry and high dimensional analyses to study immune cell phenotypes, abundance, activation states, and functions in endometrium and blood of women with and without endometriosis in different cycle phases and disease stages.

Methods: A case-control study was designed. Endometrial biopsies and blood ($n = 60$ total) were obtained from women with ($n = 20$, $n = 17$, respectively) and without ($n = 14$, $n = 9$) endometriosis in the proliferative and secretory cycle phases of the menstrual cycle. Two mass cytometry panels were designed: one broad panel and one specific for mononuclear phagocytic cells (MPC), and all samples were multiplexed to characterize both endometrium and blood immune composition at unprecedented resolution. We combined supervised and unsupervised analyses to finely define the immune cell subsets with an emphasis on MPC. Then, association between cell types, protein expression, disease status, and cycle phase were performed.

Results: The broad panel highlighted a significant modification of MPC in endometriosis; thus, they were studied in detail with an MPC-focused panel. Endometrial CD91⁺ macrophages overexpressed SIRP α (phagocytosis inhibitor) and CD64 (associated with inflammation) in endometriosis, and they were more abundant in mild versus severe disease. In blood, classical and intermediate monocytes were less abundant in endometriosis, whereas plasmacytoid

*Correspondence: linda.giudice@ucsf.edu

†Ashley F. George, Sushmita Sen, Alexis J. Combes and Linda C. Giudice contributed equally to this work.

¹ Center for Reproductive Sciences, Department of Obstetrics, Gynecology and Reproductive Sciences, University of California San Francisco, San Francisco, CA, USA

Full list of author information is available at the end of the article



dendritic cells and non-classical monocytes were more abundant. Non-classical monocytes were higher in severe versus mild disease.

Conclusions: A greater inflammatory phenotype and decreased phagocytic capacity of endometrial macrophages in endometriosis are consistent with defective clearance of endometrial cells shed during menses and in tissue homeostasis, with implications in endometriosis pathogenesis and pathophysiology. Different proportions of monocytes and plasmacytoid dendritic cells in blood from endometriosis suggest systemically aberrant functionality of the myeloid system opening new venues for the study of biomarkers and therapies for endometriosis.

Keywords: Endometriosis, Macrophages, Monocytes, Mononuclear phagocytes, SIRPα, Innate immune, CyTOF, Biomarker, Endometrium

Background

Endometriosis is a common, chronic, estrogen-dependent, inflammatory disorder affecting approximately 10% of reproductive age women, 60% with chronic pelvic pain, and 50% with infertility [1]. It is characterized by endometrial-like tissue outside the uterine cavity, arriving in the pelvis by retrograde menstruation and at distant sites by hematogenous and/or lymphatic spread [2]. Endometrial tissue at sites ectopic to the uterus results in an intense inflammatory response, neo-neuroangiogenesis, fibrosis, and scarring [1]. About 97% of women have retrograde menstruation, although most do not develop endometriosis, and while the risk of developing disease is approximately 50% genetic and 50% environmental [1], predicting who will develop symptoms remains uncertain. There are no biomarkers for endometriosis and the gold standard diagnosis is by laparoscopy. Current therapies include surgical removal of lesions or hormonal ovarian suppression, but disease recurrence and medication side-effects limit long-term symptom relief [1]. Establishment of disease has been attributed to a profound but incompletely understood dysfunction of both innate and adaptive immune responses. The aberrant immune milieu is associated with inefficient clearance of ectopic lesions, pelvic and systemic inflammation, and abnormalities in the endometrium, including alterations in the landscape and function of local immune cells [3, 4]. Understanding endometriosis-related immune dysfunction may be important in defining clinically meaningful disease phenotypes and support the development of novel diagnostic and therapeutic strategies.

Endometriosis has been called “the disease of the macrophage”, based on studies revealing a central role for macrophages in disease establishment, angiogenesis, nerve fiber development, and involvement in pain perception [5]. Recently, a mouse model of the disease demonstrated that macrophages in lesions derive from eutopic endometrium (lining the uterus), circulating monocytes, and large peritoneal macrophages [6]. Moreover, it demonstrated that endometrial macrophages are “pro-endometriosis,” as their depletion resulted in smaller

endometriotic lesions, while monocyte-derived peritoneal macrophages are “anti-endometriosis”, protecting from lesion establishment [6]. These data confirm key roles for endometrial macrophages and a possible defect in myeloid function in this disorder. Recently, we found, by RNA-Seq, that isolated endometrial macrophages from women with endometriosis have signatures of enhanced inflammation, supporting a role for these cells in the pathogenesis and pathophysiology of this disorder [7]. Molecular and cellular characterization of the human myeloid system in peripheral blood and endometrium of women with endometriosis has been limited, in part, by established methods to isolate and study these cells. Technologic advances in immunology research, including mass cytometry (i.e., *cytometry by time of flight* (CyTOF)), enable deep phenotyping of immune and other cell types. Mass cytometry enables simultaneous measurement of more than 40 proteins at single-cell resolution in a complex tissue. Herein, we have leveraged CyTOF to study human endometrium and peripheral blood immune cells (PBMCs) of those with endometriosis (cases) and without disease (controls) and in different menstrual cycle phases (estrogen-dominant proliferative phase and progesterone-dominant secretory phase). Two complementary CyTOF panels consisting of 42 and 40 phenotypic and functional markers were designed. The first, a broad immune phenotyping panel enabled resolution and comparison of endometrial immune populations. The second panel focused exclusively on phenotyping mononuclear phagocytic cells (MPC) in both endometrium and blood. The data reveal enrichment and activation of distinct populations in cases (endometriosis) and controls, menstrual cycle phases, and endometriosis disease stages and offer candidates for diagnostic and therapeutic target development.

Methods

Sample collection and processing

A total of 34 fresh endometrial tissues (Control = 14, Endometriosis = 20) and 26 blood samples (Control = 9, Endometriosis = 17) were collected from women with

and without endometriosis undergoing surgery (total $n = 60$). Clinical features of the patients (cycle phase, diagnosis, and stage of disease) are listed in Additional file 1: Table S1. Diagnosis was made by the physician and pathologists at the University of California, San Francisco (UCSF), and stage of disease was determined following the rASRM classification system (stages I and II were determined as mild and III and IV as severe stages) [8]. Women without visualized endometriosis at the time of surgery or without a history of endometriosis were defined as controls. Women with any type of cancer and/or endometrial hyperplasia were also excluded. Some patients exhibited non-malignant gynecologic disorders such as leiomyomas or uterine polyps. Cycle phase was determined by following Noyes et al. system of classification of endometrial histology [9]. Clinical features of the patients were collected only by authorized personnel by using the REDCap Database, after informed written consent. Only patients of reproductive age (18–49 years old) were included in the study. In addition, patients presenting with immune-related comorbidities, such as systemic lupus erythematosus (SLE), endometritis, or other immune disorders, were excluded, as well as those positive for HIV, HVB, and HVC. Moreover, patients were not exposed to hormone therapies for at least 3 months prior to biospecimen collection. Finally, women under any treatment containing iodine were also excluded from the study, as this element interferes with the CyTOF instrument. All samples were obtained between 2019 and 2021 under the auspices of the UCSF Institutional Review Board Proctol #: IRB#10-03964, using the WERF EPHeCT standardized protocols for tissue collection, and processing, and clinical annotation [10]. All patient data were de-identified and followed HIPAA and the Convention of the Declaration of Helsinki.

Endometrial samples

Endometrium was obtained either by endometrial biopsy using a Pipelle catheter (CooperSurgical, Trumbull, CT, USA) or from hysterectomy specimens. Tissues were placed into transport medium and processed within 5 h following collection where they were first washed with serum containing media (SCM) and then digested mechanically and enzymatically using a mix of collagenase IV and hyaluronidase, as previously described [7]. After 1 h of digestion at 37 °C under rotation, for live/dead discrimination, samples were processed for incorporation of cisplatin and fixed for further usage. Briefly, the single-cell suspension was washed with FACS/EDTA buffer (PBS supplemented with 2% FBS and 2mM EDTA). Cells were counted, and an appropriate amount of cisplatin (Fluidigm, South San Francisco, CA, USA) (25 mM per 1–6 million cells) was added to the suspension (4ml

PBS/EDTA per 1–6 million cells) for exactly 60 s at room temperature (RT). Then the cells were quenched with CyFACS (metal contaminant-free PBS (Rockland, Pottstown, PA, USA) supplemented with 0.1% BSA and 0.1% sodium azide). Finally, cells were fixed with 1.6% formaldehyde for 10 min, washed three times in CyFACS, and stored at – 80 °C until further use.

Peripheral blood mononuclear cells (PBMCs)

Blood was collected in collection tubes containing anticoagulant acid citrate dextrose (ADC) Solution B (Fisher Scientific, Hampton, NH, USA). Ficoll (Stemcell Technologies, Vancouver, Canada) was slowly added to the bottom of the blood in a falcon tube at a ratio of 2:1. The samples were then centrifuged at 2000 rpm for 30 min at RT. After centrifugation, the supernatant was removed and the PBMC layer was carefully collected. PBMCs were washed twice with FACS buffer, and the number of cells was then counted. The same protocol above was used to incorporate cisplatin, fix, and store the cells.

Panel designs

First, we designed a CyTOF broad panel to identify the important cell types in endometrial tissue of women with endometriosis compared to controls. This panel consisted of 42 markers and is shown in Additional file 2: Table S2. Then, we designed a 40-parameter CyTOF panel that includes mostly myeloid surface markers as well as functional markers, including efferocytosis and phagocytosis, activation, and inhibition markers (Additional file 2: Table S2). For the broad panel, all 42 antibodies were conjugated in house. For the myeloid panel, sixteen of the 40 antibodies required in-house conjugation to their corresponding metal isotope. Metals were conjugated according to the manufacturer's instructions (Fluidigm, South San Francisco, CA, USA). Briefly, this process comprises loading the metal to a polymer (incubation of 1 h at RT). The unconjugated antibody is transferred into a 50-kDa Amicon Ultra 500 V-bottom filter (Fisher Scientific, Hampton, NH, USA) and reduced at 37 °C with 1:125 dilution of Tris (2-carboxyethyl) phosphine hydrochloride (TCEP) (Thermo Fisher, Waltham, MA, USA) for 30 min. Then, the column is washed twice with buffer C (Fluidigm, South San Francisco, CA, USA) and the metal-loaded polymer is suspended in 200 μ l of C-buffer in the 3-kDa Amicon Ultra 500-ml V-bottom filter (Fisher Scientific, Hampton, NH, USA). The suspension is then transferred to the 50-kDa filter containing the antibody and incubated for 1.5 h at 37 °C. After the incubation time, antibodies are washed three times with W-buffer (Fluidigm, South San Francisco, CA, USA) and quantified for protein content by Nanodrop. Once the concentration was determined, the antibodies were

resuspended with Antibody Stabilizer (Boca Scientific, Dedham, MA, USA) at a concentration of 0.2 mg/ml and stored at 4 °C. The rest of the antibodies were commercially available (Fluidigm, South San Francisco, CA, USA). Optimal concentrations of all antibodies were performed by different rounds of titrations.

Barcoding and cell staining with metal antibodies

The staining protocol was optimized to use each antibody in aliquots of 6 million cells as previously described [11]. Samples were thawed and washed with FACS buffer. Then, cells were counted and since some samples had fewer than 6 million cells, they were barcoded before the staining with the antibodies, following the manufacturer's instructions (Fluidigm, South San Francisco, CA, USA). Briefly, each sample was incubated with 10 µl of each barcode and perm buffer (Fluidigm, South San Francisco, CA, USA) for 30 min at RT, and then samples were combined and split into different tubes for the first day of staining. For the staining, samples were blocked using rat, mouse, and human serum for 15 min on ice. They were then washed and stained with the primary cocktail of antibodies for 45 min at 4 °C. After this incubation time, cells were washed and fixed using 2% paraformaldehyde (PFA) diluted in CyPBS. Cells were incubated overnight at 4 °C and the next day were washed with perm buffer (Fluidigm, South San Francisco, CA, USA), washed with CyPBS, and blocked with rat and mouse serum for 15 min on ice. They were then washed, and the intracellular staining was performed. Cells were resuspended with the intracellular cocktail of antibodies for 45 min on ice and were washed and incubated for 20 min at RT with Ir-intercalator (Biolegend CNS, San Diego, CA, USA), prepared at a dilution of 1:500 in 2% fresh PFA. After the incubation time, cells were washed and kept at 4 °C overnight. Finally, on the third day, cells were washed with cell staining media (CSM, Fluidigm, South San Francisco, CA, USA), then with water, and then with cell acquisition solution (CAS, Fluidigm, South San Francisco, CA, USA) at RT. Subsequently, cells were counted, resuspended in 1 × EQTM calibration beads (Fluidigm, South San Francisco, CA, USA) and CAS and samples were run in the CyTOF[®]2 instrument (Fluidigm, South San Francisco, CA, USA).

Data processing

The fcs. files obtained from the instrument were concatenated, normalized to EQTM calibration beads, and de-barcoded using CyTOF software (Fluidigm, South San Francisco, CA, USA). This study is comprised of eight different sample groups: control (Ctrl) and endometriosis (Endo) eutopic endometrium (EM) in the proliferative (PE) and secretory (SE) phases (Ctrl_EM_PE,

Ctrl_EM_SE, Endo_EM_PE, Endo_EM_SE) and control and blood (PBMCs) in the proliferative and secretory phases (Ctrl_PBMC_PE, Ctrl_PBMC_SE, Endo_PBMC_PE, Endo_PBMC_SE). Normalized data from the broad panel were imported to FlowJo (BD, Franklin Lakes, NJ, USA) to perform manual gating, and we performed unsupervised analysis of the manually gated CD45⁺ cells. We also performed manual gating of the different populations obtained from the focused panel and 8 populations were obtained and are shown in Additional file 3: Fig. S1. Then, unsupervised analysis of the manually gated myeloid cells of interest (including macrophages, monocytes, dendritic cells, and plasmacytoid dendritic cells) was also performed. Finally, statistical analyses for specific markers and populations of the focused panel were performed by manual gating to validate the results from the unsupervised analysis. The datasets generated and analyzed during the current study are available in the Dryad repository (doi:10.7272/Q6Q52MVQ).

Data and statistical analysis

Samples included in the study

The broad panel included a total of 17 endometrial samples (4 controls in the proliferative phase, 2 controls in the secretory phase, 6 from endometriosis patients (cases) in the proliferative phase and 5 cases in the secretory phase). For the focused panel, the endometrial data included 13 control samples (9 in the PE and 4 in SE phases, respectively) and 18 samples from women with endometriosis, which correspond to 13 in the PE phase (8 mild and 5 severe stages, respectively) and 5 in the SE phase (all mild stage of disease). In the case of the PBMCs, data from the focused panel included 9 control samples (6 in the PE and 3 in the SE phase) and 17 disease samples, corresponding to 13 in the PE phase (8 mild stage and 5 severe stage) and 4 in SE phase (3 mild and one severe). Note that some samples were used for both panels, totally 60 in the study (34 endometrial tissues ($n = 20$ control and $n = 14$ endometriosis cases) and 26 blood samples ($n = 17$ controls and $n = 9$ endometriosis cases).

Downsampling cells

The broad panel included a total of 17 endometrial samples. Endometrial samples with large numbers of cells were downsized by random cell selection to a number of cells (169,599) per sample compatible with the system's memory limits and computational efficiency. The Seurat R package for single-cell analysis [12] was used to identify clusters of cells. After combining samples, a total of 2,223,274 endometrial cells were subjected to Seurat clustering, using the levels of the 42 CyTOF markers as expression value to create Seurat objects. CyTOF

clusters were identified using a shared nearest neighbor (SNN) graph [13]. Similarly, in the focused panel, 50,000 cells per sample from PBMCs were down sampled from each subject group to enable processing within memory limits and computational efficiency. On the other hand, endometrial samples in the focused panel were not down sampled as they displayed an average of 15,000 mononuclear phagocytic cells per sample after elimination of the lineage positive (CD3+, CD56+, CD66b+). Samples with less than 1000 CD45+ cells were discarded from the study and are not shown here. Due to the different origin and properties of the two tissues, two independent Seurat objects were created. A total of 355,240 endometrial myeloid phagocytic cells and 890,602 myeloid phagocytic cells from blood were subjected to Seurat clustering. The expression level of the markers from the panel were given as expression value to create Seurat objects.

As only myeloid populations were gated and analyzed, markers for other cell types were excluded from the analysis (CD45, CD3, CD56, CD66b). In addition, the expression levels of the antibodies MerTK and Er α were negative, indicating that the staining did not perform well, and these two markers were also excluded from the analyses, resulting in the inclusion of 34 markers from the panel to the final analysis. The downsampling of cells should not have resulted in any bias because cells from all subjects in the study were included in the analyses and subjected to an unbiased downsampling. Moreover, cells only from subjects with numbers of cells exceeding a chosen threshold (depending on the sample type as explained above) were downsampled.

Visualization using UMAPs colored by biological variables and technical variables

Biological variables (disease, menstrual cycle phase) and technical variables (batch/run) were visualized in different colors using the DimPlot function in the Seurat package. Because two sampling methods were used to collect the endometrial samples (hysterectomy and biopsy), we also generated and compared UMAP coordinates of the cells between the two collection methods. We concluded that they were comparable, and thus all endometrial samples were used (Additional file 4: Fig. S2A). To determine if the two sampling methods affected cell composition of each cluster, we performed *t*-test ($p < 0.05$) and compared the proportion of cells obtained by each method. We did not observe any significant differences (Additional file 4: Fig. S2B). Thus, we concluded that the tissue sampling method was not a confounder in our study.

Batch correction procedure using Harmony

After visualizing batch effects in the broad panel using DimPlot, the first and remaining group of the three

batches were treated as two batch groups and the cells were combined using the harmony batch correction function RunHarmony [14]. Similarly, samples run in batch/run 5 for the focused panel (both endometrial and PBMCs) were systematically different from the samples run in batches 1–4 (Additional file 5: Fig. S3). Therefore, samples under run 5 and the rest of the samples were treated as two separate batches that were subjected to correction using the RunHarmony function to proceed with further analysis.

Clustering of cells at different resolutions

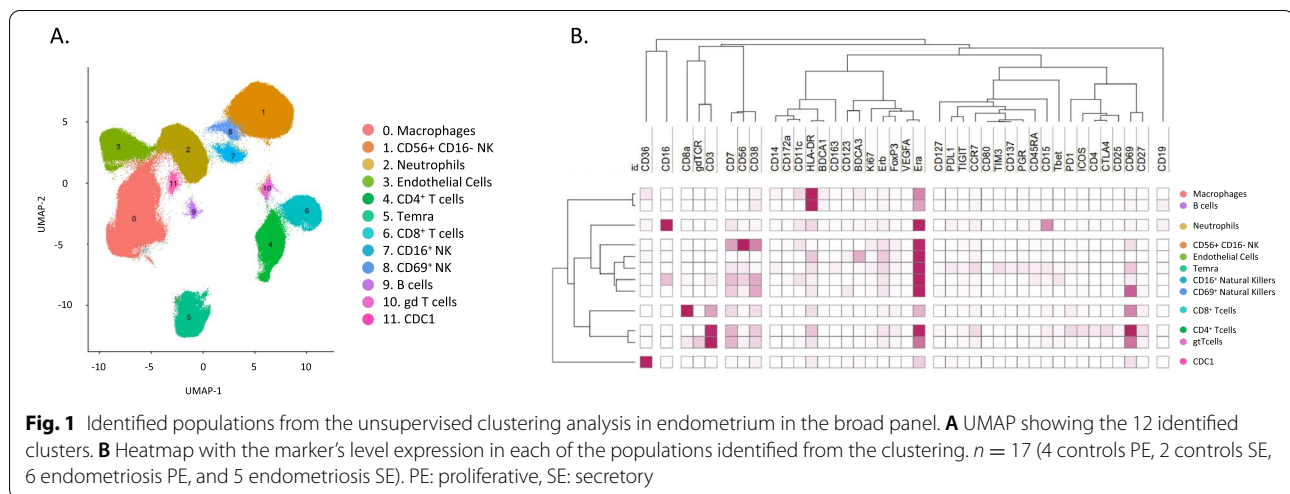
Clustering of the cells was performed using the FindClusters function (implementing the “original Louvain” algorithm) in the Seurat package at resolutions 0.01, 0.1, 0.2, 0.4, 0.8, 1, and 1.5. At each of these resolutions, the markers for each cluster were determined using the FindMarkers function in Seurat where the processing batch for each sample was encoded as a latent variable. The average expression for each marker was determined using the AverageExpression function in the Seurat. After looking at the cisplatin levels (dead cells), some clusters were removed, as they presented high levels of dead cells; also, very small clusters that contained less than 100 cells were excluded. In the broad panel, the resolution parameter was chosen to be 0.2 for endometrium. In the focused panel, the resolution parameter was chosen to be 0.4 and 0.2 for endometrium and PBMCs, respectively.

Between cluster association with disease and menstrual cycle state

A generalized linear mixed model (GLMM) (implemented in the lme4 [14] package in R with family argument set to the binomial probability distribution) was used to estimate the association between cluster membership, disease, and menstrual cycle phase. The model consisted of cluster membership as a response variable and five explanatory variables: subject as a random effect variable, variables encoding disease, menstrual cycle phase, their interaction, and a batch variable were included as fixed variables.

Between cluster association with disease stage

GLMM was also used to explore the association between cluster membership and disease stage of cells. Disease samples from patients with mild or severe stage were selected for disease stage association analysis. The model explanatory variables included subject as a random effect, disease stage, menstrual cycle, and the processing batch (for analyses involving disease samples processed across multiple batches) as fixed variables. Only proliferative phase samples were studied due to limited secretory phase samples from patients with severe disease.



Within cluster association with disease and menstrual cycle

To assess the association (per cluster) between CyTOF marker expression quantile levels and disease, menstrual cycle phase and their interaction, a linear model was fit. The tested marker expression quantile values of 25%, 50%, and 75% for each subject were estimated across all the subjects' cells. In addition to variables that capture disease status, menstrual cycle phase, and their interaction, a variable capturing the processing batch was also included as explanatory variables in the linear model.

Within cluster association with disease stage

Similarly, a linear model was used to explore the association between CyTOF marker cell expression quantile levels and disease stage. The variables included in these models are described in the section "Between cluster association with disease stage". All p -values were corrected using the false discovery rate (FDR), and a threshold of 0.05 was used to determine significance for the distribution of cells in each cluster and 0.1 for marker expression. GLMM was performed using R package lme4 [15], and linear regression was performed using the lm function in R. Only proliferative phase samples were studied.

Validation of the unsupervised analysis by manual gating

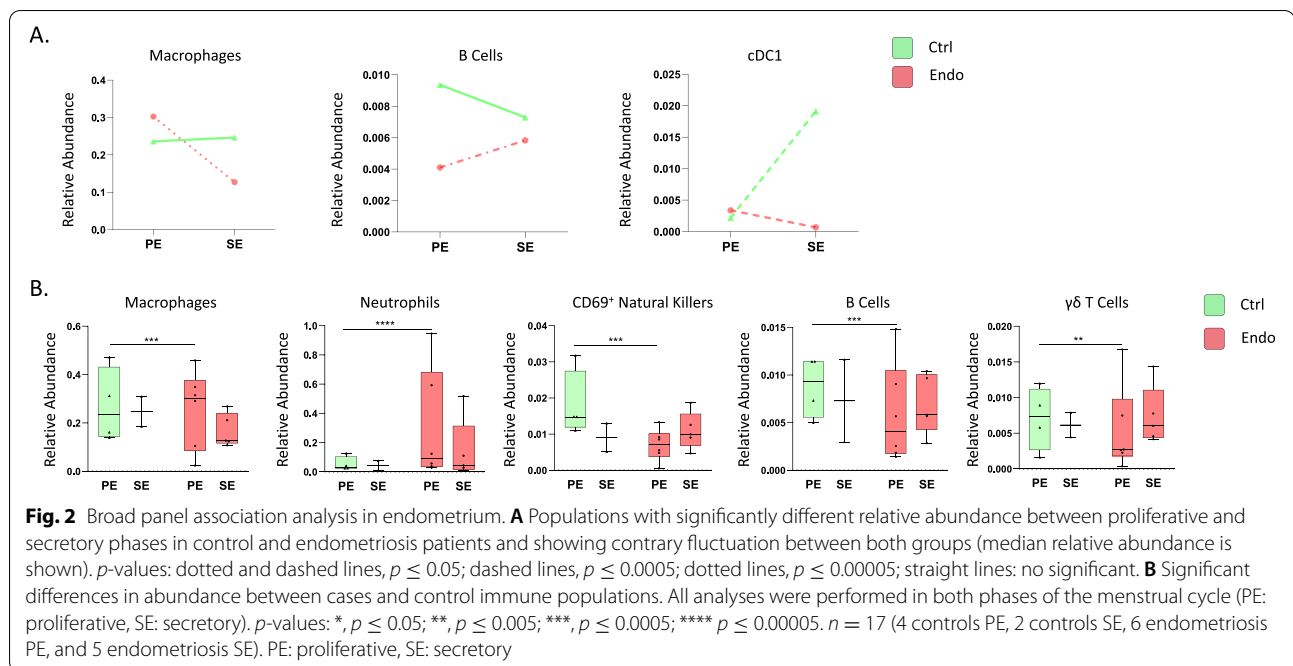
To validate the results, we manually gated the populations of interest in FlowJo and studied their abundance and marker expression. To find differences in expression between the manually gated populations, we extracted the mean signal intensity (MSI) of each marker, and its expression was compared between the different groups by t -test ($p \leq 0.05$) and multiple correction with

Benjamini-Hochberg (BH) with a false discovery rate (FDR) lower than 0.05.

Results

Broad immune phenotyping identifies differences in abundance and variation throughout the cycle in endometrial immune populations in women with and without endometriosis

Clustering analysis (which include all samples analyzed in the study; controls and cases with endometriosis in both proliferative and secretory phases of the cycle) revealed 11 distinct immune clusters and one cluster of putative endothelial cells, the latter of which has been observed to express CD45 at low levels in some tissues [16]. The 11 immune cell clusters correspond to macrophages, natural killer cells (NK), neutrophils, and subsets of CD4⁺ T cells including Temra (effector memory T cells that re-express CD45RA after antigenic stimulation), CD8⁺ T cells, CD16⁺ NK, CD69⁺ NK, B cells, $\gamma\delta$ T cells, and class I conventional dendritic cells (cDC1) (Fig. 1). Briefly, T cells were identified by the high expression of CD3. Their subsets were identified by the high expression of CD4 (T cells CD4⁺) and CD8 (T cells CD8⁺), CD45RA (Temra), and $\gamma\delta$ TCR ($\gamma\delta$ T cells). B cells were identified by the expression of CD19. Cells expressing high levels of CD15 and CD126 were classified as neutrophils. Macrophages were identified by the high expression of HLA-DR, CD11c, CD36, and CD14, and they were negative for CD3, CD56, and CD19, among others. We found three clusters of natural killer cells (NK). We identified them as they are all are negative for the lineage markers CD3 and CD14 but express different levels of CD56. In addition, the close proximity of clusters 1, 7, and 8 on the UMAP indicates similarities among the three clusters. So, to differentiate among the three NK cells subsets,



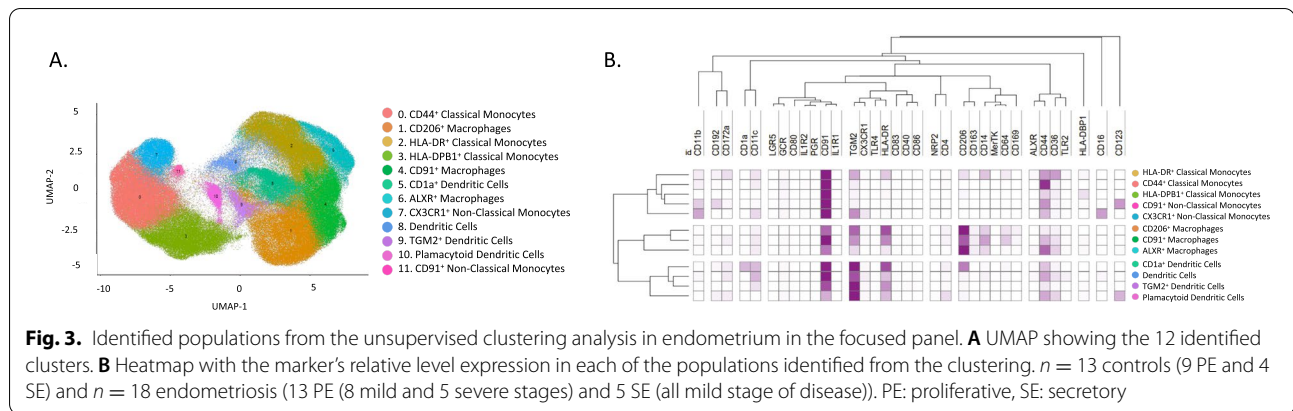
we named them with the expression of the most distinguishing markers based on the literature. First, Cluster 1 (CD56+ CD16– NK) is CD56+ and CD16–, which corresponds to infiltrating natural killers (from blood); cluster 7 (CD16+ NK) corresponds to endometrial natural killers (CD56 dim and CD16 bright, markers consistent with activation; and third, those that highly express CD69 (CD69+ NK), a marker previously described in tissue-resident NK cells [17]. Endothelial cells were defined by the high-level expression of BDCA3, as it is known that these cells highly express this marker [18, 19]. Cluster 11 was annotated and defined as cDC1 due to its expression of BDCA3, CD36, CD11c, and HLA-DR and being negative for CD3, CD4, CD14, and BDCA1, which are gold standard markers for cDC1 in humans. Nonetheless, the high BDCA3 expression in endothelial cells and the normalization across the column in the heatmap obscure the expression of BDCA3 in cluster 11 (Fig. 2b). The proportion of each population in all conditions (control and endometriosis in both phases of the cycle) is shown in Additional file 6: Fig. S4. Populations displaying significant differences in abundance between controls and cases across the menstrual cycle are presented in Fig. 2A. The distribution of all populations in both controls and cases is shown in Additional file 7: Fig. S5. In controls, the abundance of cDC1 significantly increased in the secretory phase of the cycle as did macrophages albeit insignificantly, while in women with endometriosis, both populations significantly decreased (Fig. 2A). In addition, while B cells tended to decrease in the secretory phase in

controls, this population significantly more abundant in samples acquired during the secretory phase from cases (Fig. 2A). Furthermore, we found statistically significant differences between abundance of specific populations in cases and controls. We observed increased abundance of macrophages and neutrophils in the proliferative phase and decreased CD69+ NK, B cells, and $\gamma\delta$ T cells in the proliferative phase in cases vs controls (Fig. 2B).

Increased abundance of subsets of macrophages and neutrophils in endometrium of women with endometriosis in the proliferative phase (Fig. 2B) indicates more inflammation in tissues from women with disease compared to controls. This observation suggesting that myeloid populations may be involved in disease prompted the development of a mononuclear phagocyte-focused panel to study these populations in more detail.

Mass cytometry reveals distinct subsets of mononuclear phagocyte populations in endometrium

We then combined phenotypic and functional markers of the mononuclear phagocyte populations including activation/inhibition markers, phagocytosis markers, and efferocytosis markers. By using manual gating, we first excluded T cells, NK, and granulocytes and then performed the unsupervised analysis on the remaining cells. The unsupervised clustering yielded 13 unique cell populations (Fig. 3), including one which was characterized by an absence of expression of any mononuclear phagocyte markers and was therefore excluded for further analysis, as it may be a potential B cells cluster. In this manner, we



identified 12 clusters in the endometrial tissue (analysis made with all samples; cases and controls in both proliferative and secretory phases). We found three clusters corresponding to classical monocytes ($CD44^+$ classical monocytes, $HLA-DR^+$ classical monocytes, and $HLA-DPB1^+$ classical monocytes) defined by a high expression of $CD14$ and $CD36$, and low expression of $CD16$; three macrophage clusters ($CD206^+$ macrophages, $CD91^+$ macrophages, and $ALXR^+$ macrophages) defined by the expression of $CD11c$, $CD64$, and $CD206$; two clusters of non-classical monocytes ($CX3CR1^+$ non-classical monocytes and non-classical monocytes) defined by their $CD16$ expression and low expression of $CD14$. In the case of the dendritic cells' classification, the focused panel did not contain a great number of specific markers for subsets of dendritic cells, such as $CD141$ or $CD1c$, which made more difficult their identification. However, it included $CD1a$, $CD11c$, $CD123$, $CD14$, and $CD16$ which allowed their broad identification. Consequently, we used a hybrid strategy to identify DCs subsets. We first isolated plasmacytoid dendritic cells (pDCs) using the gold standard classification of lineage negative ($CD3$, $CD56$, $CD14$, $CD16^-$, and $CD11c^-$) and expression of $HLA-DR^+$, $CD11c^-$, $CD16^-$, and $CD123^+$ markers. Regarding classical dendritic cells, we had not included in this panel the markers $BDCA1$ ($CD1c$) and $BDCA3$ ($CD141$), classical markers for $cDC2$ and $cDC1$, respectively. Nevertheless, based on the literature, $cDCs$ are $CD14dim$, and $CD11c^+$ (also shown in Additional file 3: Fig. S1), which is the case for the three clusters of dendritic cells that we have identified named dendritic cells, $TGM2^+$ dendritic cells and $CD1a^+$ dendritic cells. In addition, we added dendritic cell markers in the focused panel that we believed could be involved in endometriosis. It is well known that dendritic cells can express $CD1a^+$ [20]. This marker is believed to be an immature marker for DCs while $CD83^+$ is a marker of mature DCs. As it

was previously described that in endometrium of women with endometriosis, immature DCs ($CD1a^+$) were more abundant than $CD83^+$ mature DCs [21], these two markers were included in the focused panel. We identified a cluster (cluster 5) with high expression of $CD1a$, indicating that these may be immature dendritic cells. On the other hand, $TGM2^+$ is also expressed in DCs [22] and it is believed to be involved in dendritic cell-T cell interaction. However, it is inevitable that the relationship between those subsets and the classical $cDC1$ and $cDC2$ will need to be established. The expression levels of all markers for each population are shown in Fig. 3B and in Table 1.





Specific endometrial monocyte and macrophage subsets display distinct dynamics throughout the menstrual cycle in endometriosis patients

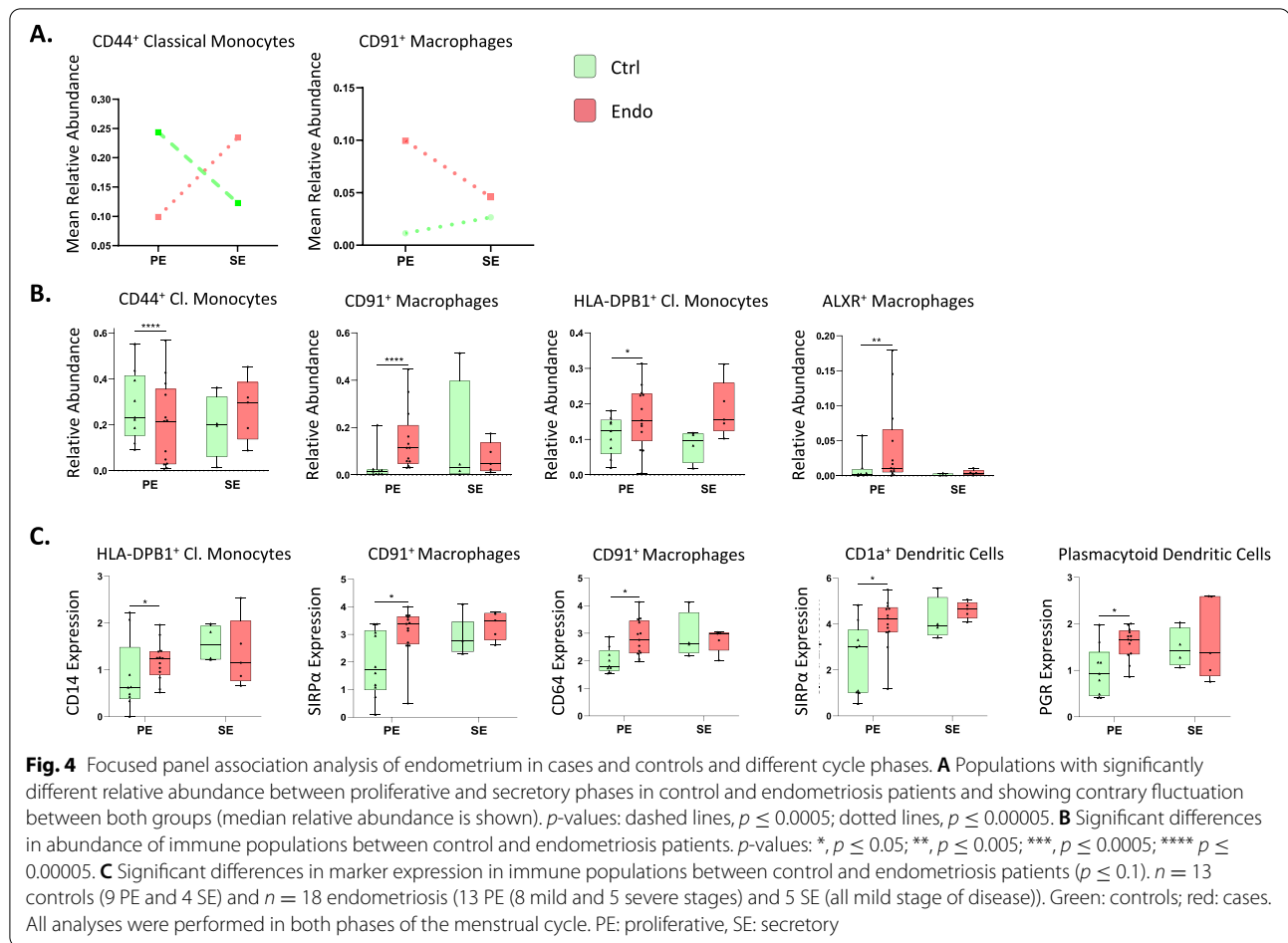
In the endometrium of controls, $CD44^+$ classical monocytes and $ALXR^+$ macrophages decreased in the secretory phase of the cycle, whereas $HLA-DR^+$ classical monocytes and $CD91^+$ macrophages increased (Additional file 8: Fig. S6). Interestingly, the opposite pattern was observed in $CD44^+$ classical monocytes and $CD91^+$ macrophages from women with endometriosis (Fig. 4A). The distribution of all identified populations with the focused panel in both groups is shown in Additional file 8: Fig. S6. These observations indicate that the specific populations have different dynamics throughout the cycle between cases and controls, suggesting different hormonal regulation of these populations in disease.

Abundance and marker expression of specific proliferative phase mononuclear phagocytic subsets differ in endometriosis patients

Association analysis revealed an increased endometrial $HLA-DPB1^+$ classical monocytes, $CD91^+$ macrophages, and $ALXR^+$ macrophages, and decreased $CD44^+$ classical

Table 1 Identified populations from the unsupervised clustering analysis obtained from the focused panel. The numbers in the parenthesis indicate the number of each cluster showed in the UMAP. Levels of expression were determined by the intensity mean of each marker in each cluster; 0–5 (–), 6–100 (+), 101–500 (++) , 501–1000 (+++) , > 1000 (++++)

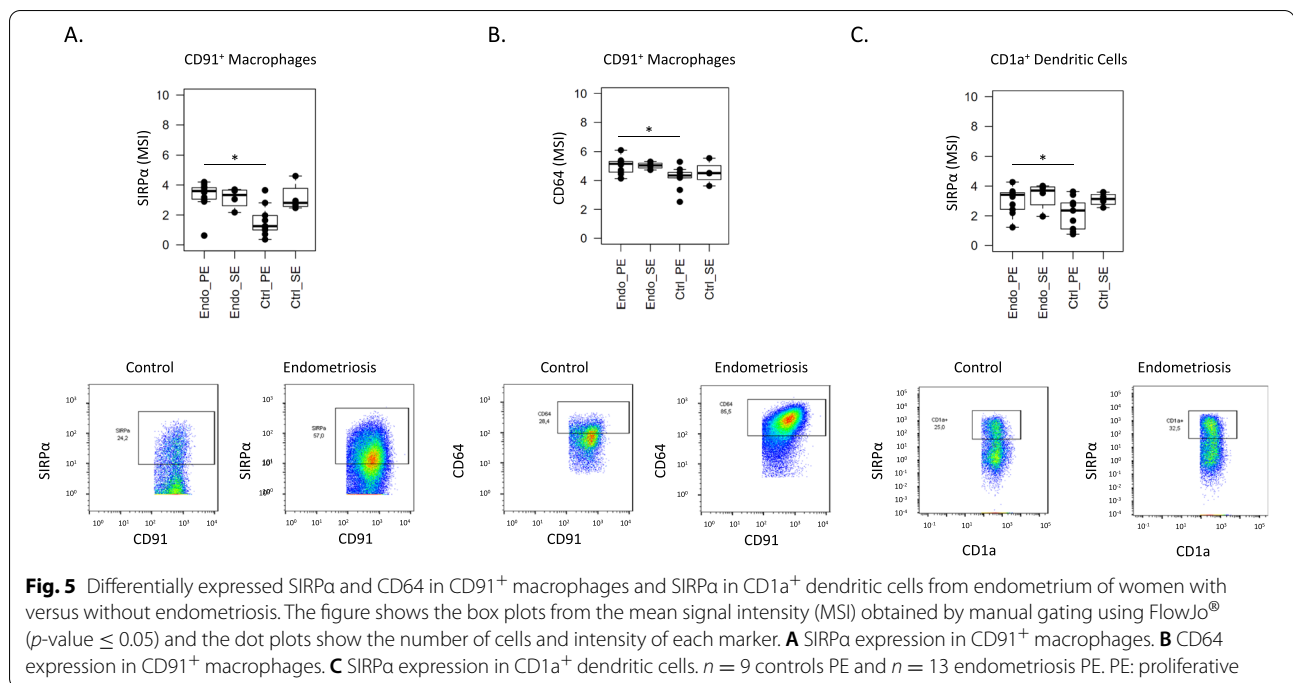
Endometrium					
Population	Subsets	Markers			
 Macrophages	(1) CD206 ⁺ Macrophages	HLA-DR+++ CD11c+ CD14++ CD11b+ CD16-	CD206++++ CD64++ CD36+ CD163+ CX3CR1+	CD44+ CD91+++ TGM2+++ CD80+ CD83+	CD172a+ CD192+ CD123-
	(4) CD91 ⁺ Macrophages	HLA-DR+++ CD11c++ CD14+++ CD11b+ CD16+	CD206++++ CD64++ CD36++ CD163+ CX3CR1+	CD44++ CD91++++ TGM2+++ CD80+ CD83+	CD172a++ CD192+ CD123+
	(6) ALXR ⁺ Macrophages	HLA-DR++ CD11c++ CD14++ CD11b+ CD16-	CD206++++ CD64+ CD36++ CD163++ CX3CR1+	CD44++++ CD91++++ TGM2++ CD80+ CD83+	CD172a+ CD192+ CD123+
 Classical Monocytes	(0) CD44 ⁺ Classical Monocytes	HLA-DR- CD11c+ CD14+ CD11b+ CD16-	CD206- CD64- CD36+ CD163- CX3CR1-	CD44++ CD91++ TGM2+ CD80- CD83-	CD172a- CD192- CD123-
	(2) HLA-DR ⁺ Classical Monocytes	HLA-DR++ CD11c+ CD14++ CD11b+ CD16-	CD206++ CD64+ CD36++ CD163+ CX3CR1+	CD44++ CD91+++ TGM2++ CD80- CD83+	CD172a++ CD192+ CD123-
	(3) HLA-DPB1 ⁺ Classical Monocytes	HLA-DR+ CD11c+ CD14+ CD11b+ CD16-	CD206+ CD64+ CD36+ CD163- CX3CR1+	CD44++ CD91++++ TGM2+ CD80+ CD83+	CD172a+ CD192+ CD123-
 Non-Classical Monocytes	(7) CX3CR1 ⁺ Non-Classical Monocytes	HLA-DR- CD11c+ CD14- CD11b+ CD16+	CD206- CD64- CD36+ CD163+ CX3CR1+	CD44+ CD91+ TGM2+ CD80- CD83-	CD172a- CD192- CD123-
	(11) CD91 ⁺ Non-Classical Monocytes	HLA-DR- CD11c- CD14- CD11b+ CD16-	CD206- CD64- CD36- CD163- CX3CR1-	CD44+ CD91++ TGM2+ CD80- CD83-	CD172a- CD192+ CD123+
 Dendritic Cells	(8) Dendritic Cells	HLA-DR+ CD11c+ CD14+ CD11b+ CD16+	CD206+ CD64+ CD36+ CD163- CX3CR1+	CD44++ CD91++ TGM2++ CD80- CD83-	CD172a+ CD192- CD123-
	(5) CD1a ⁺ Dendritic Cells	HLA-DR+++ CD11c++ CD14+ CD11b+ CD16+	CD206+++ CD64+ CD36+ CD163- CX3CR1+	CD44++ CD91++++ TGM2++++ CD80+ CD83+	CD172a+ CD192+ CD123-
	(9) TGM2 ⁺ Dendritic Cells	HLA-DR+++ CD11c++ CD14+ CD11b- CD16-	CD206+ CD64- CD36+ CD163- CX3CR1+	CD44++ CD91++++ TGM2++++ CD80+ CD83+	CD172a+ CD192+ CD123-
	(10) Plasmacytoid Dendritic Cells	HLA-DR++ CD11c- CD14- CD11b- CD16-	CD206+ CD64- CD36++ CD163- CX3CR1+	CD44++ CD91++ TGM2+++ CD80- CD83-	CD172a+ CD192+ CD123++



monocytes in cases versus controls in the proliferative phase (Fig. 4B). Within some populations, association analysis revealed several markers significantly different between cases and controls (Fig. 4C). For example, CD14 expression on HLA-DPB1⁺ classical monocytes was increased in the proliferative phase in cases versus controls. Interestingly, the anti-phagocytosis marker SIRP α (CD172a) was increased on phagocytic CD91⁺ macrophages and CD1a⁺ dendritic cells in cases versus controls in the proliferative phase, suggesting decreased phagocytic capacity of these populations in endometriosis patients. In addition, an increase in expression of CD64 was found in proliferative phase in CD91⁺ macrophages from cases, indicating higher inflammation. PGR was more highly expressed in pDCs in cases versus controls in the proliferative phase. These results suggest that specific phagocytic cell subsets may have altered functions in endometrium of women with endometriosis. The expression of the significant markers between cases and controls in all cell types during the proliferative phase is shown in Additional file 9: Table S3.

Endometrial CD91⁺ macrophages and CD1a⁺ dendritic cells display phenotypes suggesting reduced phagocytic capacity and CD91⁺ macrophages display an inflammatory bias in cases versus controls

Unsupervised analyses showed an increase of SIRP α in CD91⁺ macrophages and in CD1a⁺ dendritic cells, as well as increased levels of CD64 in CD91⁺ macrophages. By differential expression analyses on manually gated mononuclear phagocytic subsets, we found that, in the proliferative phase, a greater frequency of CD91⁺ macrophages in endometrium of women with endometriosis express SIRP α compared to controls (Fig. 5A) and they have higher expression levels of CD64 in the proliferative phase of the menstrual cycle (Fig. 5B), corroborating the results observed with the unsupervised analysis. We also validated by manual gating that SIRP α was overexpressed by CD1a⁺ dendritic cells in endometrium of cases versus controls in the proliferative phase (Fig. 5C). These results suggest inhibition of the phagocytic capacity of endometrial CD91⁺ macrophages and CD1a⁺ dendritic cells and an inflammatory bias among CD91⁺ macrophages in women with endometriosis.



Distinct endometrial mononuclear phagocyte populations display disease-stage-specific abundance in the proliferative phase

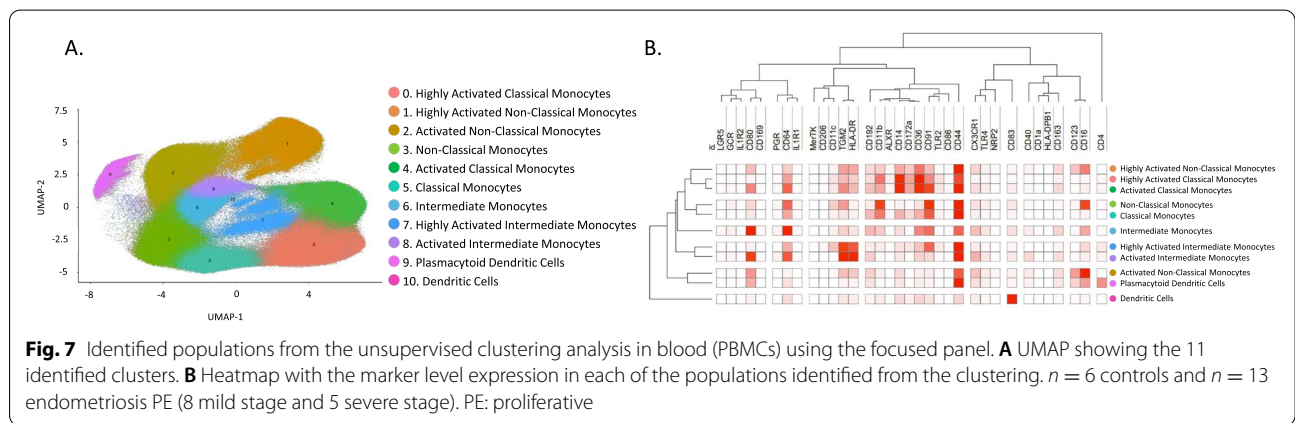
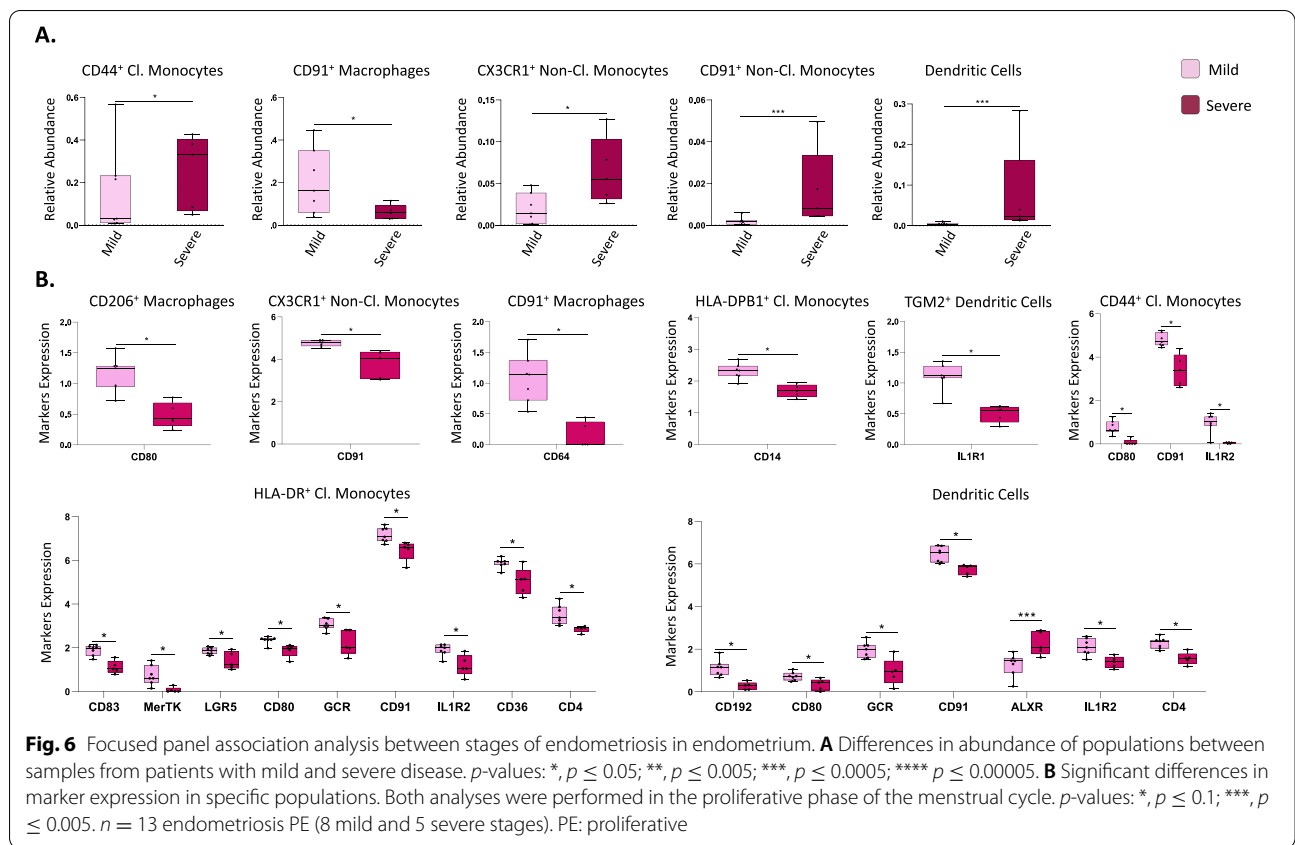
In the setting of severe versus mild disease, a higher proportion of endometrial CD44⁺ classical monocytes, CX3CR1⁺ and CD91⁺ non-classical monocytes, and dendritic cells were observed, as well as lower levels of CD91⁺ macrophages (Fig. 6A). Notably, and as shown above, CD91⁺ macrophages and CD44⁺ monocytes appear to have different dynamics throughout the cycle in controls and endometriosis patients, as well as different proportions between the two groups, suggesting that they may be key components for the pathophysiology of the disease.

In addition, association analyses of marker expression levels across populations were conducted to identify functional phenotypes and possible differences and roles in the setting of severe versus mild stage disease. This revealed several markers significantly differentially expressed in some endometrial immune populations depending on disease stage (Fig. 6B). CD206⁺ macrophages had higher CD80 expression and CD91⁺ macrophages had higher CD64 expression levels in endometrium from women with mild versus severe disease, suggesting higher activation and inflammatory phenotype of these populations in mild disease. Similarly, HLA-DPB1⁺ classical monocytes had higher expression of CD14 and activated classical monocytes (CD44⁺) showed an increase of CD80, CD91, and IL1R2 expression, also indicating higher activation in mild disease. Highly

activated classical monocytes (HLA-DR⁺) displayed increased CD83, MerTK, LGR5, CD80, GCR, CD91, IL1R2, CD36, and CD4, showing also higher activation in mild stage. CX3CR1⁺ non-classical monocytes showed an increase in CD91 in patients with mild endometriosis. Dendritic cells had higher expression of CD192 (CCR2), CD80, GCR, CD91, IL1R2, and CD4 and a decrease of ALXR, suggesting that some of these cells are monocyte-derived dendritic cells and that they are more activated in mild than in severe disease. Finally, TGM2⁺ dendritic cells presented a higher expression of IL1R1 in endometrium of women with mild versus severe disease. Taken together, these results indicate that there is more activation in specific immune populations in mild disease when compared to severe disease, suggesting more inflammation endometrium in early stages of endometriosis.

Distinct mononuclear phagocyte populations in peripheral blood are associated with endometriosis disease status





As the data in endometrium revealed differences in macrophages, some monocytes, and dendritic cells in women with versus without endometriosis, PBMCs were then analyzed using the focused panel to evaluate possible comparable dysregulation and if these populations could be an indicator of disease. Because only differences in the proliferative phase of the cycle were observed in endometrium, the analysis was restricted to samples from this cycle phase. After the clustering analysis, 11 populations were identified, corresponding to three clusters of classical monocytes (classical

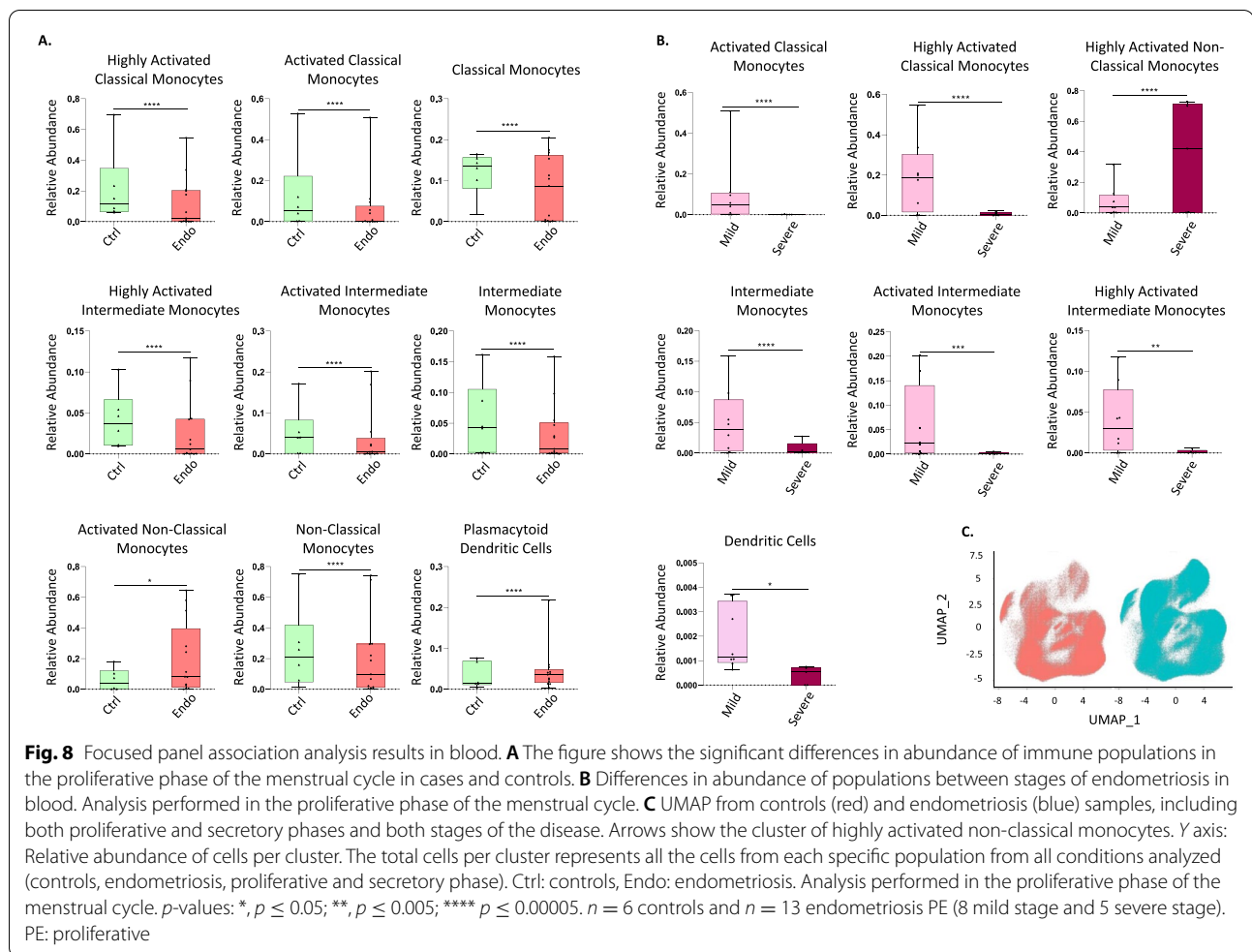


monocytes, activated classical monocytes, and highly activated classical monocytes) defined by their expression of CD14 (high) and CD16 (low) and the expression of activation markers, such as HLA-DR and CD44; three clusters of intermediate monocytes (intermediate monocytes, activated intermediate monocytes, and highly activated intermediate monocytes) also identified by the expression of both CD14 and CD16 and activation markers; three clusters of non-classical

monocytes (non-classical monocytes, activated non-classical monocytes, and highly activated non-classical monocytes) defined by their expression of CD14 (low) and CD16 (high) and activation markers; one cluster of dendritic cells, defined by their expression of HLA-DR, CD11c, among others; and one cluster of pDCs, identified by their high expression of CD123. The specific expression of all markers from the panel in each population are shown in Fig. 7 and Table 2.

Table 2 Identified populations in peripheral blood from the unsupervised clustering analysis obtained using the focused panel. The numbers in the parenthesis indicate the number of each cluster showed in the UMAP. Levels of expression were determined by the intensity mean of each marker in each cluster; 0–5 (–), 6–100 (+), 101–500 (++) , 501–1000 (+++) , > 1000 (++++)

PBMC					
Population	Subsets	Markers			
 Classical Monocytes	(5) Classical Monocytes	HLA-DR+	CD163+	CD80+	TLR4+
		CD11c+	CD64+	CD44++	CD83+
		CD14+	CD36+	CD91+	MerTK-
		CD11b+	CD192+	CD172a+	CD40-
		CD16+	TGM2+	CX3CR1+	TRL2+
	(4) Activated Classical Monocytes	HLA-DR++	CD163++	CD80++	TLR4+
		CD11c+	CD64++	CD44+++	CD83+
		CD14+++	CD36+++	CD91+++	MerTK+
		CD11b++	CD192++	CD172a++	CD40+
(0) Highly Activated Classical Monocytes	HLA-DR+++	CD163+	CD80+	TLR4+	
	CD11c++	CD64++	CD44+++	CD83+	
	CD14++++	CD36++++	CD91+++	MerTK-	
	CD11b+++	CD192++	CD172a++	CD40-	
	CD16+	TGM2++	CX3CR1+	TLR2++	
 Intermediate Monocytes	(6) Intermediate Monocytes	HLA-DR+	CD163+	CD80++	TLR4+
		CD11c+	CD64++	CD44+	CD83+
		CD14+	CD36++	CD91++	MerTK-
		CD11b+	CD192+	CD172a-	CD40+
		CD16+	TGM2+	CX3CR1+	TLR2+
	(8) Activated Intermediate Monocytes	HLA-DR++	CD163+	CD80++	TLR4+
		CD11c-	CD64++	CD44++	CD83+
		CD14+	CD36+	CD91+	MerTK-
	(7) Highly Activated Intermediate Monocytes	CD11b+	CD192+	CD172a-	CD40+
CD16+		TGM2++	CX3CR1+	TLR2+	
HLA-DR+++		CD163+	CD80+	TLR4+	
CD11c++		CD64++	CD44+++	CD83+	
 Non-Classical Monocytes	(3) Non-Classical Monocytes	HLA-DR-	CD163-	CD80+	TLR4+
		CD11c+	CD64+	CD44++	CD83+
		CD14-	CD36+	CD91+	MerTK-
		CD11b+	CD192+	CD172a-	CD40-
		CD16+	TGM2+	CX3CR1+	TLR2-
	(2) Activated Non-Classical Monocytes	HLA-DR++	CD163++	CD80++	TLR4+
		CD11c+	CD64++	CD44+++	CD83+
		CD14+++	CD36+++	CD91+++	MerTK-
		CD11b++	CD192++	CD172a++	CD40+
(1) Highly Activated Non-Classical Monocytes	CD16++	TGM2++	CX3CR1++	TLR2+	
	HLA-DR+++	CD163++	CD80++	TLR4+	
	CD11c+	CD64++	CD44+++	CD83+	
	CD14++	CD36+++	CD91++	MerTK-	
 Dendritic Cells	(10) Dendritic Cells	CD11b++	CD192++	CD172a++	CD40+
		CD16++	TGM2++	CX3CR1++	TLR2+
		HLA-DR++	CD163+	CD80++	TLR4+
		CD11c+	CD64++	CD44++	CD83++++
		CD14++	CD36++	CD91++	MerTK-
	(9) Plasmacytoid Dendritic Cells	CD11b+	CD192+	CD172a-	CD40+
		CD16++	TGM2+	CX3CR1+	TLR2-
		HLA-DR+	CD163+	CD80++	TLR4+
		CD11c-	CD64+	CD44++	CD83+
		CD14+	CD36+	CD91+	MerTK-



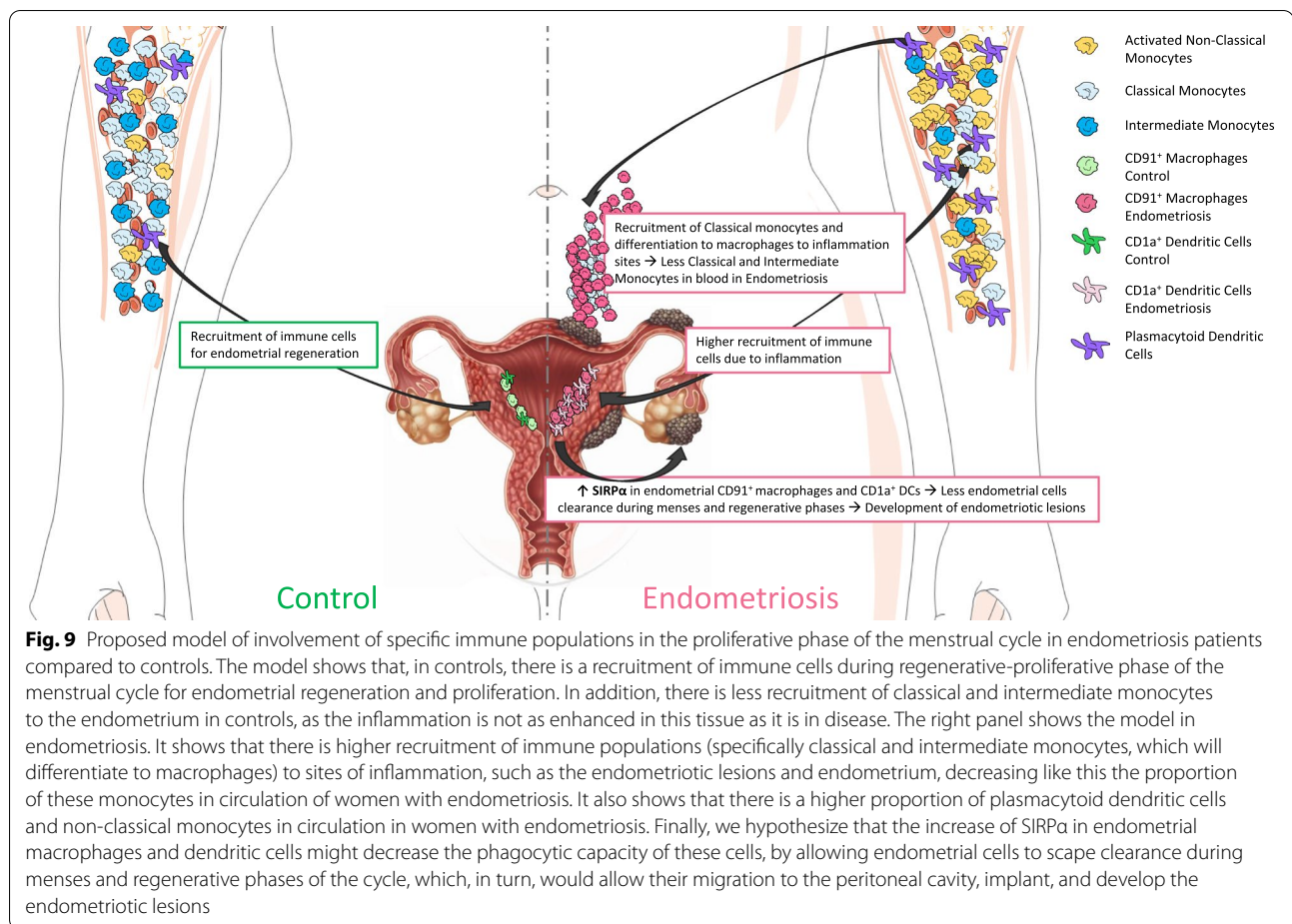
Association analysis performed in the proliferative phase of the menstrual cycle revealed an increased proportion of activated non-classical monocytes and pDCs in blood from women with endometriosis compared to controls and a decrease of classical monocytes, intermediate monocytes, and non-activated non-classical monocytes (Fig. 8A). However, significant differences in markers between controls and cases were not found, suggesting that previous differences in marker expression found in endometrium may be tissue specific.

Finally, to evaluate if there could be an association of immune populations in blood with severity of the disease, association analysis of stages of endometriosis in blood were performed. The results showed that classical monocytes (highly activated and activated), intermediate monocytes (intermediate monocytes; activated and highly activated), and dendritic cells are more abundant in peripheral blood from women with mild versus severe disease, suggesting that there is recruitment of monocytes to sites of inflammation in women

with endometriosis. In contrast, highly activated non-classical monocytes were significantly higher in the setting of severe disease (Fig. 8B), and, interestingly, this population was considerably more abundant in endometriosis than in control patients (Fig. 8C), which could serve as a biomarker of disease and, specifically, severity of endometriosis.

Discussion

The data herein provide strong support for a compromised innate immune system in endometrium and blood of women with endometriosis. Mass cytometry has revolutionized the cytometry field, allowing simultaneously labeling and analyzing cells of interest at the single-cell level with a greater number of antibodies than traditional flow cytometry. To our knowledge, we are the first group to deep phenotype endometrial immune cells using CyTOF, although others have used this technique in peritoneal fluid and blood [23] and in menstrual effluent [24]. Herein, we used two complementary CyTOF panels comprised of 42 and 38 (after exclusion of non-mononuclear phagocytes)



markers that enabled deep phenotyping of endometrium and PBMCs from women with and without endometriosis to better understand the role of these populations in disease. To note, previous studies did not use a mononuclear phagocyte-focused panel, which allowed us to identify more detailed differences. Using the broad panel, we identified significantly higher abundance of endometrial macrophages and neutrophils in endometriosis patients compared to controls. We also showed that the dynamics throughout the menstrual cycle of macrophages, dendritic cells, and B cells had contrary direction between both phases in disease and controls. As differences were mainly observed in mononuclear phagocytes, which were also the most abundant among the CD45⁺ cells, we further pursued deep phenotyping of this populations and discovered differences in controls and cases in different hormonal milieu (cycle phases). As the sample size in the secretory phase was small and significant differences were not found in this phase, we focused on the proliferative phase. The latter is estrogen-dominant and is analogous to the initial inflammatory phase for repairing the endometrium after menses, where pro-inflammatory macrophages play a vital role in wound-healing [25].

Thus, this phase provides valuable information to study the immune populations in endometrial function.

Deep immunophenotyping of mononuclear phagocytes indicates decreased phagocytic capacity of macrophages and dendritic cells in endometrium of women with endometriosis

Our results showing higher abundance of endometrial macrophages in the proliferative phase in women with versus without endometriosis are in accordance with other studies [26]. Also, overexpression of MCP-1 (CCL2) and IL-1 β in endometrium of women with endometriosis [27] suggests increased infiltration of monocytes that differentiate to macrophages in this tissue in women with disease (Fig. 9). Our results show that CD91⁺ macrophages are more abundant and have different dynamics throughout the cycle in cases versus controls. CD91 participates in the efferocytosis of apoptotic cells—a crucial function during endometrial shedding. Notably, we found that endometrial CD91⁺ macrophages and CD1a⁺ dendritic cells overexpress SIRP α —which acts to inhibit efferocytosis by these cells—in women

with endometriosis compared to controls. Healthy cells express “don’t-eat-me” signals, exposing different markers, such as CD47, that, when exposed, are recognized by SIRP α , and prevent engulfment by initiating a cascade of events leading to the inhibition of phagocytosis. Such engulfment is promoted by the calreticulin/CD91 pathway as an “eat-me” signal. In many cancers, calreticulin is exposed in the cell surface that would indicate an “eat-me” signal. However, this process does not occur in cancer, and why this molecule is exposed in cancerous cells is still unclear [28]. We found that macrophages that overexpress SIRP α in endometriosis are CD91⁺. Even if they express the latter, these observations suggest that their phagocytic capacity may be compromised by concomitant overexpression of SIRP α , suggesting that endometrial cells in women with endometriosis behave similarly to cancer cells, sending signals that interfere with the CD91 pathway in macrophages preventing efferocytosis. Thus, the overexpression of this marker in specific myeloid cells may be a consequence of aberrant functionality of eutopic endometrial cells in women with endometriosis. Xie et al. demonstrated that in vitro cultured macrophages treated with endometrial homogenates from women with endometriosis had significantly increased SIRP α expression, not observed when the macrophages were treated with homogenates of endometrium from women without disease [29], also suggesting that signals from eutopic endometrium affect the phagocytic capacity of macrophages. Another study evaluated the effect of this pathway in endometrial stromal cells from endometrium of women with endometriosis and in endometriosis lesions in vitro [30]. Co-culture of PBMCs and lesion-derived stromal cells resulted in upregulation of SIRP α in macrophages, further supporting paracrine endometrial cell interactions in macrophage dysfunction and disease establishment. Notably, we found that endometrial CD1a⁺ dendritic cells also overexpress SIRP α in women with versus those without endometriosis, indicating that other endometrial phagocytic cells may also be dysregulated in women with endometriosis. Decreased phagocytic capacity in macrophages and dendritic cells may allow aberrant endometrial cells to escape immunologic surveillance during tissue shedding, leading to establishing pelvic endometriosis (Fig. 9). Sampson’s theory of the origin of endometriosis proposes that endometrial cells shed during menses survive and migrate to the peritoneal cavity through retrograde menstruation, where they implant and develop endometriotic lesions [31]. Our results, together with the above studies, suggest that endometrial macrophages have defective phagocytic capacity in women with versus without endometriosis, opening opportunities for mining new targets to prevent development and/or progression of the disease as well

as endometrial dysfunction. Expression of calreticulin in endometrial cells in women with endometriosis and the effects in the calreticulin/CD91 pathway warrant further study to confirm this paradigm.

In addition, our findings that CD91⁺ endometrial macrophages are more abundant and overexpress CD64 in women with endometriosis and in mild versus severe stage disease suggest a more enhanced pro-inflammatory phenotype in mild disease due to the expression of CD64. Therapeutic targeting of CD64 expressed on pro-inflammatory macrophages, proposed for other chronic inflammatory diseases, may be useful in the context of endometriosis [32].

Immunophenotyping suggests higher infiltration of circulating monocytes to sites of inflammation in women with endometriosis

Discovery herein has revealed that in addition to endometrial immune populations, specific PBMC populations differ in women with versus without endometriosis. Importantly, classical and intermediate monocytes are in lower abundance and pDCs and activated non-classical monocytes are more abundant in blood from women with versus without disease. These findings are in line with a recent study that described decreased phagocytic function of monocytes in blood from patients with endometriosis before surgery, and normalization after lesion removal, compared to controls undergoing surgery but without endometriosis [33]. In addition, proliferation of endometrial cells in vitro from women with endometriosis is significantly enhanced by blood monocytes, whereas monocytes from healthy patients inhibit their proliferation [34], indicating factors influencing these cells act as enhancers or suppressors of endometriotic lesion development. Our results that classical and intermediate monocytes are less abundant in blood from patients with endometriosis are consistent with increased recruitment of monocytes to sites of inflammation, e.g., to the peritoneal cavity, where endometriotic lesions are commonly found, and to the uterine endometrium, where we also observed a higher proportion of macrophages in women with disease in the proliferative phase. In addition, these populations may have less phagocytic function and thus play a role in deficient clearance of ectopic endometrial tissue, resulting in endometriotic lesion development (Fig. 9). While the above studies by others did not differentiate findings in the setting of mild and severe disease or different types of monocytes, our results show that this effect is more profound in severe disease, where there are significantly less circulating classical and intermediate monocytes than in mild disease, suggesting this defective function is enhanced in more advanced disease.

Abundance of specific mononuclear phagocytes in blood are putative biomarkers of disease and severity of endometriosis

Notably, we found an increase of activated non-classical monocytes and pDCs in blood of women with endometriosis versus controls and that the former were more associated with advanced stage disease. Suen et al. demonstrated in a murine model that IL-10 secreted from pDCs promotes endometriotic lesion development through aberrant angiogenesis early in disease establishment [35]. Our results show that pDCs are associated with disease but not stage. This is in contrast to the mouse model, where the association with early disease establishment can be assessed experimentally, unlike human endometriosis where the evolution cannot be reliably assessed. It is well known that pDCs are involved in some autoimmune diseases and play a pivotal role in the development of autoantibodies through impaired type I interferon (type I INF) production [36], enhancing systemic autoimmunity [37]. Endometriosis is a chronic inflammatory disease that shares many similarities with autoimmune disorders [38], including production of autoantibodies [3]. A recent meta-analysis by Shigesaki et al. found a greater risk of autoimmune diseases in patients with endometriosis, including systemic lupus erythematosus, Sjögren's syndrome, rheumatoid arthritis, celiac disease, multiple sclerosis, inflammatory bowel disease, autoimmune thyroid disorders, and Addison's disease [39]. In addition, more severe endometriosis is being associated with concomitant autoimmune diseases [40]. Thus, it is of great interest to determine the precise role of pDCs in endometriosis pathophysiology and the role of systemic cytokines, such as INF family members, to better understand common immunopathology between endometriosis and autoimmune diseases. Interestingly, in the autoimmune disorder neuromyelitis optica spectrum disorder (NMOSD), non-classical monocytes have a higher frequency than in controls in blood [41]. Non-classical monocytes are believed to be patrolling and anti-inflammatory innate immune cells. However, their roles in chronic diseases, such as in multiple sclerosis or systemic lupus erythematosus, are less clear as their functions can be protective as well as positively associated with disease burden [42]. Given our observation of their greater abundance in blood of women with endometriosis and, specifically, in those with severe disease, and as endometriosis is a chronic inflammatory disorder, further study of the functional roles of this population and mining biomarkers of disease severity warrants further investigation. Although the patients in the current study did not have autoimmune comorbidities, further analysis of abundance and function of non-classical monocytes and pDCs, as well as their cytokine

production in patients with endometriosis, having or not concomitant autoimmune diseases, is of interest, especially as the role of these populations in endometriosis remains unresolved.

Some of the limitations of the study include a limited sample size, especially in the secretory phase of the menstrual cycle. As mentioned above, this may be a reason why we found only differences in the proliferative phase. Although in this study, we show differences in the latter, a larger sample size in all phases would further confirm differences highlighted by our discovery cohort. Another limitation of the study is that the focused panel did not contain a B cell-specific marker. As we observed differences in B cell frequency by using the broad panel, indication that B cells may also have a role in disease would require further investigation. Along the same line, while we were able to identify coarsely dendritic cell populations, additional choice of markers specific for this population would be needed to deeply characterize and distinguish between known subsets such as cDC1 and cDC2. Therefore, the design of the focused panel caused some limitations for cell identification of specific cell subtypes. Finally, due to the differential proteomic profile between blood and endometrium-associated classical monocytes, we cannot directly relate them between the different biospecimen compartments. We therefore have maintained a different nomenclature of monocytes between endometrium and blood to avoid unsupported conclusions. It would be important to relate these different classical monocytes in the different compartments in the future, which may require experiments using animal models to dissect classical monocyte ontogeny.

Although we had some limitations in the study, to our knowledge, this cohort size represents the largest cohort of endometrial samples from women with and without endometriosis analyzed by mass cytometry reported to date. Applying two different panels enabled us to identify populations that could be involved in endometriosis, and the second panel allowed deep phenotyping the MPC system at the protein level for the first time in eutopic endometrium of women with and without endometriosis. Considering the heterogeneity of the disease and the immune complexity, further single-cell studies, e.g., using more focused panels for other immune populations and endometrial cells, will help to better understand the immune system in endometriosis.

Conclusions

The data presented herein support that endometrial CD91⁺ macrophages and CD1a⁺ dendritic cells of women with endometriosis display a decreased phagocytic capacity compared to controls. If this is a consequence of aberrant endometrial cell functions or a defect on the immune

system, per se, awaits further investigation. In addition, classical and intermediate monocytes are less abundant in blood from women with endometriosis, suggesting higher recruitment of these populations to sites of inflammation and disease lesions, with current evidence demonstrating defective phagocytic function in the tissues and in the circulation. Finally, pDCs and activated non-classical monocytes are more abundant in endometriosis, with the latter being even higher in severe disease, which could serve as a biomarker of disease severity in blood. Overall, we conclude that the mononuclear phagocyte system is compromised in endometrium and peripheral blood of patients with endometriosis. The results of our study open alternative venues for developing new diagnostic and therapeutic targets and strategies for identifying and treating subtypes of this enigmatic disorder.

Abbreviations

ADC: Acid citrate dextrose; BH: Benjamini-Hochberg; BSA: Bovine serum albumin; Ctrl: Control; CyTOF: Cytometry by time of flight; EDTA: Ethylenediaminetetraacetic acid; Endo: Endometriosis; ESE: Early secretory; FACS: Fluorescent activated cell sorting; FDR: False discovery rate; GLMM: Generalized linear mixed model; INF: Interferon; LSE: Late secretory; MPC: Mononuclear phagocytic cells; MSE: Mid secretory; MSI: Mean signal intensity; PBMCs: Peripheral blood mononuclear cells; PE: Proliferative; PFA: Paraformaldehyde; Rpm: Revolutions per minute; RT: Room temperature; SCM: Serum containing media; SE: Secretory; SNN: Shared nearest neighbor; TCEP: Tris (2-carboxyethyl) phosphine hydrochloride.

Supplementary Information

The online version contains supplementary material available at <https://doi.org/10.1186/s12916-022-02359-4>.

Additional file 1: Table S1. Samples used in the study. Endo: endometriosis; PE: proliferative; SE: secretory; MSE: mid secretory, LSE: late secretory; N/A: not applicable.

Additional file 2: Table S2. CyTOF panels used in the study. Left: broad panel, right: focused panel.

Additional file 3: Fig. S1. Manual gating strategy for the focused panel. The figure shows an example of the dot plots obtained using FlowJo in endometrial cells.

Additional file 4: Fig. S2. Endometrial sampling methods. A) The figure shows UMAPs of the two methods used for endometrial tissue collection, biopsy (red) and hysterectomy (blue). The left panel shows a UMAP with the overlap between the two techniques and the right panel the split UMAPs for each technique. $n=17$ endometrial biopsies and $n=17$ hysterectomies. B) The graph shows the proportion of cells in each cluster obtained by the different sampling methods.

Additional file 5: Fig. S3. Batch effects derived from different runs. The figure shows UMAPs representing the distribution of the cells from the runs in the CyTOF instrument for both endometrium (top panel) and PBMCs (bottom panel). The figure shows the UMAPs before (left panel) and after (right panel) batch correction. Red: runs 1 to 4; blue: run 5.

Additional file 6: Fig. S4. Proportion of endometrial immune populations identified by using the broad panel. The figure shows the proportion of each population in the ring graphs and the percentage of each population is also shown in each condition of study. Ctrl_PE ($n=4$), Ctrl_SE ($n=2$), Endo_PE ($n=6$), Endo_SE ($n=5$). Ctrl: control, Endo: endometriosis, PE: proliferative, SE: secretory.

Additional file 7: Fig. S5. Fluctuation of all endometrial immune populations identified in the broad panel. A) Differences in abundance

of populations throughout the menstrual cycle in control samples. B) Differences in abundance of populations throughout the menstrual cycle in samples from women with endometriosis. pValues: *, $pVal \leq 0.05$; **, $pVal \leq 0.005$; ***, $pVal \leq 0.0005$; **** $pVal \leq 0.00005$. $n=17$ (4 controls PE, 2 controls SE, 6 endometriosis PE, 5 endometriosis SE). PE: proliferative, SE: secretory.

Additional file 8: Fig. S6. Fluctuation of all endometrial immune populations identified in the focused panel. A) Differences in abundance of populations throughout the menstrual cycle in control samples. B) Differences in abundance of populations throughout the menstrual cycle in samples from women with endometriosis. pValues: *, $pVal \leq 0.05$; **, $pVal \leq 0.005$; ***, $pVal \leq 0.0005$; **** $pVal \leq 0.00005$. $n=13$ controls (9 PE and 4 SE) and $n=18$ endometriosis (13 PE (8 mild and 5 severe stages) and 5 SE (all mild stage of disease)). (PE: proliferative, SE: secretory).

Additional file 9: Table S3. Expression of the significant markers between endometriosis and controls in all cell types in endometriosis versus controls from the focused panel. Significant values are highlighted in grey. Endo: endometriosis; Ctrl: controls; BH: Benjamini-Hochberg adjusted p -value.

Acknowledgements

We acknowledge Tristan Coureau, Nayvin Chew, Stanley Tamaki, Bushra Samad, Gabriella Fradgiadakis, for their help in teaching some of the used protocols. We also acknowledge the NIH S10 1S100D021822-01 grant from the UCSF Flow CoLab.

Authors' contributions

JV: processing of samples, design of panels, acquisition, analysis, and interpretation of data, drafting, and reviewing the article; SS: processing of samples and acquisition of data; RT: data analysis, drafting, and reviewing the article; MGS: data analysis, drafting, and reviewing the article; DK: processing of samples, design of panels, acquisition of data; JV: design of panels and reviewing the article; AFG: experimental design and optimization of protocols, and reviewing the article; KCV: collection of samples; JCI: interpretation of data and reviewing the article; NRR: experimental design, optimization of protocols, and reviewing the article; AJC: design of panels, analysis, and interpretation of data, drafting, and reviewing the article; LCG: experimental design, data interpretation, drafting, writing, and reviewing and editing the article. All authors read and approved the final manuscript.

Funding

This research was supported by the NIH Eunice Kennedy Shriver National Institute for Child Health and Human Development P50 HD055764 (LCG), the Kerfuffle Foundation (LCG), the ImmunoX CoPilot, and the Research Fund Award, UCSF Center of Reproductive Sciences.

Availability of data and materials

The datasets generated and analyzed during the current study are available in the Dryad repository (doi:10.7272/Q6Q52MVQ).

Declarations

Ethics approval and consent to participate

Specimens were obtained from the UCSF/NIH Human Endometrial Tissue Bank under IRB approval (IRB#10-02786) from 2019 to 2021. Written informed consent was obtained from all participants.

Consent for publication

Not applicable.

Competing interests

The authors declare that they have no competing interests. LCG: consultant for Myovant Sciences, ForEndo Pharmaceuticals, NextGen Jane, and Cematix, Inc.

Author details

¹Center for Reproductive Sciences, Department of Obstetrics, Gynecology and Reproductive Sciences, University of California San Francisco, San Francisco, CA, USA. ²Bioliquid Innovative Genetics S.L., Barcelona, Spain. ³Gladstone

Institutes, San Francisco, CA, USA. ⁴Department of Urology, University of California San Francisco, San Francisco, CA, USA. ⁵San Jose State University, San Jose, CA, USA. ⁶Bioinformatic Core Gladstone Institutes, San Francisco, CA, USA. ⁷UCSF CoLabs, University of California of San Francisco, San Francisco, CA, USA. ⁸ImmunoX initiative, University of California of San Francisco, San Francisco, CA, USA. ⁹Department of Medicine, University of California of San Francisco, San Francisco, CA, USA. ¹⁰Department of Pathology, University of California of San Francisco, San Francisco, CA, USA.

Received: 20 December 2021 Accepted: 29 March 2022

Published online: 15 April 2022

References

- Zondervan KT, Becker CM, Koga K, Missmer SA, Taylor RN, Viganò P. Endometriosis. *Nat Rev Dis Primers*. 2018;4:9. <https://doi.org/10.1038/s41572-018-0008-5>.
- Wang Y, Kristen Nicholes I-M. The origin and pathogenesis of endometriosis. *Physiol Behav*. 2020;24:71–95.
- Riccio L d GC, Santulli P, Marcellin L, Abrão MS, Batteux F, Chapron C. Immunology of endometriosis. *Best Pract Res Clin Obstet Gynaecol*. 2018;50:39–49.
- Vallvé-Juanico J, Houshdaran S, Giudice LC. The endometrial immune environment of women with endometriosis. *Hum Reprod Update*. 2019;25(5):564–91.
- Capobianco A, Rovere-Querini P. Endometriosis, a disease of the macrophage. *Front Immunol*. 2013;28(4):9.
- Hogg C, Panir K, Dhani P, Rosser M, Mack M, Soong D, et al. Macrophages inhibit and enhance endometriosis depending on their origin. *Proc Natl Acad Sci U S A*. 2021;118(6):e2013776118.
- Vallvé-Juanico J, Santamaria X, Vo KC, Houshdaran S, Giudice LC. Macrophages display proinflammatory phenotypes in the eutopic endometrium of women with endometriosis with relevance to an infectious etiology of the disease. *Fertil Steril*. 2019;112:1118–28.
- Theron E, Shaw GB, Action S. Revised American Society for Reproductive Medicine classification of endometriosis: 1996. *Soc Work (South Africa)*. 2007;43:283–90.
- Noyes RW, Hertig AIRJ. Dating the endometrial biopsy. *Fertil Steril*. 1950;1:3–25.
- Rahmioglu N, Fassbender A, Vitonis AF, Tworoger SS, Hummelshoj L, D'Hooghe TM, et al. World Endometriosis Research Foundation Endometriosis Phenome and Biobanking Harmonization Project: III. Fluid bio-specimen collection, processing, and storage in endometriosis research. *Fertil Steril*. 2014;102:1233–43.
- Ma T, Luo X, George AF, Mukherjee G, Sen N, Spitzer TL, et al. HIV efficiently infects T cells from the endometrium and remodels them to promote systemic viral spread. *Elife*. 2020;9:1–24.
- Satija R, Farrell JA, Gennert D, Schier AF, Regev A. Spatial reconstruction of single-cell gene expression data. *Nat Biotechnol*. 2015;33:495–502.
- Levine JH, Simonds EFBSCD. Data-driven phenotypic dissection of AML reveals progenitor-like cells that correlate with prognosis. *Cell*. 2015;162:184–497.
- Korsunsky I, Millard N, Fan J, Slowikowski K, Wei K, Baglaenko Y, et al. Fast, sensitive, and accurate integration of single cell data with Harmony. *Nat Method*. 2020;16:1289–96.
- Bates D, Mächler M, Bolker BM, Walker SC. Fitting linear mixed-effects models using lme4. *J Stat Softw*. 2015;67:1–48.
- Bischoff J, Casanovas G, Wylie-Sears J, Kim DH, Bartko PE, Guerrero JL, et al. Whit and RAL. CD45 expression in mitral valve endothelial cells after myocardial infarction. *Physiol Behav*. 2016;176:100–6.
- Hashemi EMS. Tissue-resident NK cells: development, maturation, and clinical relevance. *Cancers (Basel)*. 2020;12:1553.
- Van De Wouwer M, Collen D, Conway EM. Thrombomodulin-protein C-EPCR system integrated to regulate coagulation and inflammation. *Arterioscler Thromb Vasc Biol*. 2004;24:1374–83.
- Martin FA, Murphy RP, Cummins PM. Thrombomodulin and the vascular endothelium: Insights into functional, regulatory, and therapeutic aspects. *Am J Physiol Heart Circ Physiol*. 2013;304:1–25.
- Chang C-CJ, Wright A, Punnonen J. Monocyte-derived CD1a + and CD1a – dendritic cell subsets differ in their cytokine production profiles, susceptibilities to transfection, and capacities to direct Th cell differentiation. *J Immunol*. 2000;165:3584–91.
- Schulke L, Berbic M, Manconi F, Tokushige N, Markham R, Fraser IS. Dendritic cell populations in the eutopic and ectopic endometrium of women with endometriosis. *Hum Reprod*. 2009;24:1695–703.
- Kim JH, Jeong EM, Jeong YJ, Lee WJ, Kang JS, Kim IG, et al. Transglutaminase 2 on the surface of dendritic cells is proposed to be involved in dendritic cell-T cell interaction. *Cell Immunol*. 2014;289:55–62.
- Guo M, Bafiligil C, Tapmeier T, Hubbard C, Manek S, Shang C, et al. Mass cytometry analysis reveals a distinct immune environment in peritoneal fluid in endometriosis: a characterisation study. *BMC Med*. 2020;18:1–16.
- Schmitz T, Hoffmann V, Olliges E, Bobinger A, Popovici R, Nößner E, et al. Reduced frequency of perforin-positive CD8+ T cells in menstrual effluent of endometriosis patients. *J Reprod Immunol*. 2021;148:1–32.
- Wynn TA, Vannella KM. Macrophages in tissue repair, regeneration, and fibrosis. *Immunity*. 2016;44:450–62.
- Vallvé-Juanico J, Houshdaran S, Giudice LC. The endometrial immune environment of women with endometriosis. *Hum Reprod Update*. 2019;25:565–92.
- Jolicoeur C, Boutouil M, Drouin R, Paradis I, Lemay A, Akoum A. Increased expression of monocyte chemotactic protein-1 in the endometrium of women with endometriosis. *Am J Pathol*. 1998;152:125–33.
- Boada-Romero E, Martínez J, Heckmann BL, Green DR. Mechanisms and physiology of the clearance of dead cells by efferocytosis. *Nat Rev Mol Cell Biol*. 2020;21:398–414.
- Xie Q, He H, Wu YH, Zou LJ, She XL, Xia XM, et al. Eutopic endometrium from patients with endometriosis modulates the expression of CD36 and SIRP-α in peritoneal macrophages. *J Obstet Gynaecol Res*. 2019;45:1045–57.
- Liu Y, Li M, Wei C, Tang L, Sheng Y, Liu Y, et al. TSP1-CD47-SIRPα signaling facilitates the development of endometriosis by mediating the survival of ectopic endometrium. *Am J Reprod Immunol*. 2020;83:0–3.
- Sampson JA. Peritoneal endometriosis, due to the menstrual dissemination of endometrial tissue into the peritoneal cavity. *Am J Obstet Gynecol*. 1928;15:101–10.
- Akinrinmade OA, Chetty S, Daramola AK, Islam MU, Thepen T, Barth S. CD64: an attractive immunotherapeutic target for m1-type macrophage mediated chronic inflammatory diseases. *Biomedicine*. 2017;5:1–18.
- Lukács L, Kovács AR, Pál L, Szűcs S, Kóvér Á, Lampé R. Phagocyte function of peripheral neutrophil granulocytes and monocytes in endometriosis before and after surgery. *J Gynecol Obstet Hum Reprod*. 2021;50(4):101796.
- Braun DP, Muriana A, Gebel H, Rotman C, Rana N, Dmowski WP. Monocyte-mediated enhancement of endometrial cell proliferation in women with endometriosis. *Fertil Steril*. 1994;61:78–84.
- Suen JL, Chang Y, Shiu YS, Hsu CY, Sharma P, Chiu CC, et al. IL-10 from plasmacytoid dendritic cells promotes angiogenesis in the early stage of endometriosis. *J Pathol*. 2019;249:485–97.
- Huang X, Dorta-Estremera S, Yao Y, Shen N, Cao W. Predominant role of plasmacytoid dendritic cells in stimulating systemic autoimmunity. *Front Immunol*. 2015;6:1–6.
- Martensen PM, Vestergaard AL, Knudsen UB. Type I interferon in chronic virus infection and endometriosis. *Trends Immunol*. 2017;38:542–57.
- Nothnick WB. Treating endometriosis as an autoimmune disease. *Fertil Steril*. 2001;76:223–31.
- Shigeshi N, Kvaskoff M, Kirtley S, Feng Q, Fang H, Knight JC, et al. The association between endometriosis and autoimmune diseases: a systematic review and meta-analysis. *Hum Reprod Update*. 2019;25:486–503.
- Stella VV, Roberta V, Noemi S, Enrico P, Diana D, Jessica O, et al. Concomitant autoimmunity may be a predictor of more severe stages of endometriosis. *Sci Rep*. 2021;11:1–6. <https://doi.org/10.1038/s41598-021-94877-z>.
- Kong BS, Kim Y, Kim GY, Hyun JW, Kim SH, Jeong A, et al. Increased frequency of IL-6-producing non-classical monocytes in neuromyelitis optica spectrum disorder. *J Neuroinflammation*. 2017;14:1–13.
- Narasimhan PB, Marcovecchio P, Hamers AAJ, Hedrick CC. Nonclassical monocytes in health and disease. *Annu Rev Immunol*. 2019;37:439–56.

Publisher's Note

Springer Nature remains neutral with regard to jurisdictional claims in published maps and institutional affiliations.